Nonlinear Interactive Analysis of Concrete Piled-Raft

التحليل الغير خطى المتبادل للبشة الخازوقية الخرسانية

Dr. Bayoumy, A. H., Eng. Wahid Ali, Dr. Mahmoud El-Meligy
Faculty of Engineering , Mansoura University, Egypt.

ملخص البحث

لقد إزداد استخدام اساسات اللبشة الخرسانية المرتكزة جزئيا على خوازيق فى العقدين الأخيرين وذلك نظرا لجدوى هذا النوع من الأساسات من الناحية الإقتصادية حيث تقاوم الأحمال الإنشائية عن طريق الخوازيق بالإضافة الى التربة تحت اللبشة الخرسانية. وتعتمد نسبة الحمل المنقول عن طريق الخوازيق الى الحمل المنقول عن طريق التربة تحت اللبشة على عدة عوامل منها: الجساءة النسبية للبشة ، مقاومة القص للتربة تحت اللبشة

يعتبر سلوك التربة بشكل عام سلوك غير خطى، وهذا البحث يقدم تحليل إنشائى فراغى لاخطى للبشة خرسانية ترتكز على خوازيق، ويعتبر الهدف الأساسى من هذا البحث هو دراسة التأثير المتبادل بين الخوازيق والتربة واللبشة الخرسانية ، وقد تمت هذه الدراسة بإستخدام برنامج ANSYS والذى أتاح إمكانية عمل تحليل لاخطى شمل اللاخطيه الناتجة من خواص المواد ومن التغير فى الشكل الهندسى ومن التغير فى حالة سطح التلامس بين التربة والمنشأ.

وقد قدمت نتائج البحث فكرة عن توزيع الأحمال بين مجموعة الخوازيق والتربة أسفل اللبشة الخرسانية وعن قيمة حمل كل خازوق من هذه المجموعة وعن عزوم الإنحناء على الخازوق عند اتصاله باللبشة الخرسانية وذلك لأنواع الخوازيق المختلفة وكذلك توزيع العزوم فى اللبشة والهبوط أسفل اللبشة وقد عرضت النتائج فى شكل منحنيات

ABSTRACT:

The piled raft foundation has shown growing applicability in the last two decades as an economic foundation type, where the structural loads are carried partly by the piles and partly by the contact stresses under the raft. The ratio of the load carried by piles to that carried directly by the contact stresses under raft depends on many factors. Among these factors are the relative rigidity of the raft, the shear strength of the soil under the raft, the shear strength of the soil at the pile tip, the frictional stresses along the piles, and the piles settlement. The investigation the effect of these factors requires reliable finite element model that takes into consideration the nonlinear soil behaviour and the interaction between soil, piles, and raft. In this article, two 3-D nonlinear finite element models of piled raft foundation are adopted. In the first model, the interface elements are placed between the piles and soil, as well as between the raft and soil. In the second model, the interface elements are placed between the piles and the soil only and a gap is formed between the raft and the soil (free standing cap). The soil is modeled using Drucker-Prager yield criteria while the piles and the raft are treated as a linear elastic material. The proposed models are applied to piled raft resting on medium clay while the piles are rested on medium dense sand. The results reflect, the interaction among the piles, raft and soil. The study shows the effect of the contact between the soil and the raft on the pile loads and raft moment and deflection.

INTRODUCTION

In the complex models as the piled raft foundation model, the choice of the

Accepted September 9, 2006

appropriate method of analysis is very important for design purposes. In fact, the method of analysis affects directly the response of the structural elements. The piled raft foundation model is studied using different methods. The method of subgrade reaction is studied by Desai, Kuppusamy, Alameddine [11], and Abo-Ouf [13]. This method neglects the interaction between adjacent piles which affects the pile settlement, pile load, and deflection and bending of the raft. Moreover, it neglects any fixation between the raft and pile heads. The methods which are based on Mindlin's equations are studied by Butterfield and Benerjee [3], Poulos and Davias [4], and Kuwabra [5]. These methods consider the raft to be either rigid or perfectly flexible, i.e., they can not deal with a pile group connected at the heads by a raft of actual stiffness. Sawko [6] used a standard frame analysis program which may model two-dimensional problem. However, this method represent a special case and has two main limitations. First, soil strain is considered to be in the elastic range. Secondly it neglect pile-to-pile interaction effects. The finite element analysis of pile foundation has been presented by many investigators. The power of the finite element method lies in its capability to model complicated conditions, represent non-linear stress/strain behavior of the soil. In addition, it may represent geometrical nonlinearity, and simulate relative displacements between pile and soil, and shear strength of soil at interface (status nonlinearity). Desai and Holloway [7] have presented an idealization of the interface layer between the soil and the structure for axisymmetric finite element model of axially loaded pile embedded in soil. Jeong, Kim, Briaud [8] have presented finite element model of piled raft foundation to study the down drag on friction and end bearing of the pile group. They consider the surrounding soil as linear elastic material and then as an elasto-plastic material. Shabana [9] has presented finite element model of concrete pile raft foundation to study the frictional stress distribution on the pile in pile group and the interaction between pile, soil, and raft. He consider the nonlinearity of material, nonlinearity of geometry, and nonlinearity of status by using interface elements between the soils and the structure. However, his study is limited to soft clay and medium clay as soil underneath the piled raft. The main objects of the present study are to reach an analysis method that can give the actual straining action for all elements of the piled concrete raft foundation model and study the interaction among the soil, piles, and raft.

GENERAL CONSIDERATIONS

The nonlinear analysis of the soil/structure interaction can be modeled to satisfy physical conditions between the soil and the structure by using the interface (contact) elements between the soil and the structure. These elements are special elements which can simulate the layer of soil at interface and represent the stress state for any point at the interface with its mode. This analysis is more complicated, since they include not only material and geometric nonlinearity but also the state of nonlinearity at the interface between the soil and structure such as slip and gap.

MODES OF THE INTERFACE

The modes of an interface under static and dynamic loading are stick (bonding), sliding, separation, rebonding, and interpenetration of one material into its neighbor. Each of these modes and their constitutive models are discussed[10].

Stick (bonding) Mode

In the stick (bonding) mode there is no relative motion under shear stress (τ) which is associated with the attempt of slipping at interface. The typical interface data indicates

that. the shear limit for bonding is dependent in some fashion on the interface normal pressure."

The experimental data shows that the critical shear stress limit for sliding at interface is governed by a coulomb – type criterion which is represented by a linear function of the normal pressure for rather large range of interface pressure as:

For stick (bonding) state the function

$$F(\sigma_n, \tau)<0.0 \qquad (1)$$

Where σ_n = interface normal stress (has negative value in compression),

τ = interface shear stress,

Slip (sliding) Mode

The sliding mode occurs when the shear stress exceeds a certain yield stress and σ_n remains compressive. In this case equation (1) becomes

$$F(\sigma_n, \tau)=0.0 \qquad (2)$$

Equation (2) represents the Coulomb friction model. This model defines an equivalent interface shear stress τ , at which sliding on the surface begins, as a function of interface normal stress σ_n (contact pressure). The equivalent interface shear stress τ will increase with the increase of interface normal stress up to a certain value at which, regardless of the magnitude of the interface normal stress, sliding will occur. This value is defined as the maximum equivalent interface shear stress. A reasonable upper estimate of a maximum equivalent interface shear stress for many materials is $\sigma_y/\sqrt{3}$ where σ_y is the Von Mises yield stress.

Separation (debonded) Mode

In separation mode normal stress σ_n tends to be tensile. The normal stress during the transition from the stick (bonding) to the separation states can change from an initial compressive to zero to tensile. But the tensile stresses are not allowed between the structure and the soil. This can be treated simply in the analysis. If the tensile normal stress exists on the interface. this will be an indication of a gap forming between the two material surfaces and materials are no longer coupled through the interface. This is simulated by zeroing the interface stress and the constitutive laws, i.e., there are not any friction or normal stresses.

Rebonded Mode

Rebonded mode occurs when the normal stress σ_n changes to compression. Once the normal stress σ_n becomes compression. this an indication of no gap between the two material surfaces and materials are coupled through the interface and the constitutive laws are reactivated. Hence. the interface returns to bonding state as mentioned before.

Interpenetration Mode

The interpenetrating mode occurs when one of the two interface materials interpenetrates into its neighbor. This mode is associated with either stick or sliding mode. The value of interpenetration of one material into its neighbor depends on the normal stiffness of the interface elements and the normal stresses on the plane of interface. It independent on the friction constants which are used in coulomb low. All contact problems require a stiffness between the contact surfaces. ANSYS program (ANSYS 2001) estimates a default value for contact stiffness based on the material properties of the underlying deformable elements as shown in Fig. 1.

The presented model in this paper can be described simply as a concrete raft slab supported by piles and the soil in which the piles are impeded in as shown in Fig. 2. It is required to make an idealization for the concrete raft by shell elements, piles by solid elements, the soil strata by solid elements, and the interface between the structure (raft and piles) and the soils by three-dimension surface-to-surface interface (contact) elements which are believed to be the best for the considered model. The main

features must be satisfied for each element, three-dimension element, nonlinearity, plasticity, and large displacement. Several element types are found in ANSYS library [11]. SOLID45 element is used to model the soils and the piles. SHELL181 element is used to model the concrete raft. TARGE170 and CONTA173 elements are used to model the interface between soil and the structure elements. TARGE170 is used for target surface and CONTA173 is used for contact surface.

METHODOLOGY

Nonlinear Analysis Solution

The finite element code ANSYS which includes material, geometrical, and status (contact) nonlinearity is used in the analysis. The displacement-based finite element method has been employed in this study. The procedure of this method depends on solving number of simultaneous linear equations. The general equation of the linear finite element method in a matrix form is:

$$F = KU \qquad (3)$$

where, F= nodal forces vector, K= stiffness matrix, U= nodal displacements vector.

In the soil/structure interaction problems, the nonlinear analysis is required to satisfy some physical conditions. The material, geometrical, and status (contact) nonlinearity have been taken into consideration. The nonlinear structure behavior cannot be represented directly with such a set of linear equations. Briefly speaking, the procedure of nonlinear solution is performed using Eq. (3) by adopting a series of successive small incremental linear solutions and assuming that the externally applied loads are described as a function of time. At completion of each incremental solution, the adjustment of the stiffness matrix has been performed to reflect the nonlinear changes in structural stiffness before proceeding to the next load increment.

More specifically, the basic problem in a general nonlinear analysis is to find the state of equilibrium of a body corresponding to the applied loads. Assuming that the externally applied loads are described as a function of time, the equilibrium conditions of a system of finite elements representing the body under consideration can be expressed at any time as [12]

$$^{t}R - {}^{t}F = 0 \qquad (4)$$

where

^{t}R = externally applied nodal forces at time t.

^{t}F = the nodal point forces that correspond to the element stresses at this time t.

$$^{t}R = {}^{t}R_B + {}^{t}R_S + {}^{t}R_C, \qquad (5)$$

$$^{t}F = \sum_{m} \int_{V(m)} {}^{t}B^{(m)T} \, {}^{t}\tau^{(m)} \, dV^{(m)} \qquad (6)$$

$^{t}R_B$ = body force vector,

$^{t}R_S$ = surface force vector,

$^{t}R_C$ = concentrated load vector,

$^{t}B^{(m)T}$ = transposed of the strain-displacement matrix for element m at time t.

$^{t}\tau^{(m)}$ = the stresses on the element m at time t, and $V^{(m)}$ = volume of the element m.

In general large deformation analysis, the stresses and the volume of the body at time t are unknown. When the analysis includes path-dependent nonlinear geometric or material conditions, or time-dependent phenomena, the equilibrium relations in Eq. (4) need be solved for the complete time range of interest. This is carried out using a step-by-step incremental analysis. The basic approach in an incremental step-by-step solution is to assume that the solution for the discrete time t is known, and that solution for the discrete time $t + \Delta t$ is required. Where Δt is a suitably chosen time increment. Hence, considering Eq. (4) at time $t + \Delta t$ one has;

$$^{t+\Delta t}R - {}^{t+\Delta t}F = 0 \qquad (7)$$

Since the solution ^{t}F is known at time t, one can write;

$$^{t+\Delta t}F = F + {}^{t}F \qquad (8)$$

Where F is the increment in nodal forces corresponding to the increment in the

stresses from time t to time t +Δt. The vector F can be approximated using a tangent stiffness matrix at time t, ^{t}K as the following:

$$F = {}^{t}KU \qquad (9)$$

where

^{t}K= stiffness matrix at time t which corresponds to the geometric and material condition at time t, and U = vector of incremental nodal displacement.

Substituting (8) and (9) into (7) we obtain

$$ {}^{t}KU = {}^{t+\Delta t}R - {}^{t}F \qquad (10)$$

Eq. (10) can be solved for U and an approximation to the displacement $^{t+\Delta t}U$ at time t +Δt can be calculated. Then an approximation to the stresses and corresponding nodal forces at time t +Δt can be evaluated. Before proceeding to next time increment, one or more iteration is necessary until the solution of Eq. (7) is obtained to sufficient accuracy.

ILLUSTRATION EXAMPLE

Based on a parametric study, the plan dimensions of soil are taken 38.0×38.0 m and its depth is taken 32.0 m. The soil underneath the raft is medium clay and its depth is equal to 14.4m, while the bearing soil is medium sand and its depth is equal to 17.6m, see Fig. 2. For simplicity, the applied load is taken as a uniform vertical load on the whole raft. Only, one quarter of the model is solved due to symmetry. The cross-sectional area of the pile is taken square 0.5X0.5m. The plan dimensions (2Yx2Y) of the raft are 14.0X14.0m with overhang is 0.5m. The center-to-center distance of the piles S to the side length D (spacing ratio) is taken 5.0. The pile slenderness ratio L/D is equal to 32.0.The modulus of elasticity of concrete is equal to 2.1×10^{6} t/m^{2} while its Poisson's ratio is 0.2 and density is 2.5 t/m^{3}. The modulus of elasticity of soil along the pile shaft (medium clay) is equal to 3000 t/m^{2} while its Poisson's ratio is 0.3, density is 1.8 t/m^{3}, cohesion is 5.0 t/m^{2}, and angle of internal friction is 15°. The modulus of elasticity of bearing soil (medium sand) is equal to 6000 t/m^{2} while its Poisson's ratio is 0.35, density is 1.8 t/m^{3}, cohesion is zero, and angle of internal friction is 35°. Three-dimension contact elements are placed at the interface between soil and piles, and soil and raft. The interface adhesion between soil and concrete is 2.5 t/m^{2}, and angle of friction between medium clay soil and concrete is 12°. Fig. 3, shows the meshing of the two models. In the first model (see Fig. 3-a.) a contact layer is placed between the raft and the underneath soil and the total number of elements of the model are 22653 elements. In the second model (see Fig. 3-b.) a gab is placed between the raft and the underneath soil only in order to ensure a free standing cap concept. The total number of elements of the second model are 22221 elements. The unsymmetrical matrix system of the solver is used since the non-associated flow rule with Coulomb law produces unsymmetrical matrix. To give more accuracy, the adjustments have been performed by full-Newton-Raphson iterative solution[12].

PILE LOADS

In piled raft foundation the raft transmits the load to the piles and the underneath soil. The piles loads are resisted by end bearing stresses from the bearing soil (medium sand) and skin friction stresses from the surrounding soil. So the type of surrounding soil and the structural component may affect piles loads. This section presents the effect of the raft relative rigidity t/S on piles loads. Also the effect of the contact pressure under raft or the cap status is presented.

Effect of Raft Reltive Rigidity t/S on the Piles Loads

Fig. 4 shows the effect of raft relative rigidity t/S on the percentage of the pile load with respect to the total piles loads at Pt/Ptmax. 21%, Pt/Ptmax. 55%, and

Pt/Ptmax .= 100%. Where Pt is the total load applied to the structure (own weight and the raft load) and Ptmax is the maximum value of the total load applied to the structure. The figure presents the results for each pile. It is observed that, for the outer piles the increase in t/S increases the percentage of the pile load. However, the effect on the corner pile, i.e. pile P11, is more significant than that on the external piles as pile P12 and P13. Conversely, the increase in t/S results in decrease in the pile load for inner piles. However, the effect on the pile P33 is more significant than that on the other inner piles. It is worth repeating, however, that the above-mentioned behaviour is limited to the case of uniform load on the raft. It should be kept in mind that there is a symmetry about the main diagonal along the piles P11, P22, and P33. This symmetry causes the results of piles P12, P13, and P23,respectively, to be the same as that of pile P21, P31, and P32.

Effect of relative rigidity of the piled raft t/S on the point and friction resistance of the pile

Figs. 5, 6, and 7 show a comparison between two cases of raft relative rigidity t/S on the percentage of the point load and friction load for piles P11, P13, and P33 respectively with the progress of loading. The continuous curves represent the percentage of the resistance for the first case in which t/S equal to 0.24 and dash curves represent the percentage of the resistance for the second case in which t/S equal to 0.48, with the pile load (by ton). Generally speaking the behavior of the three piles are approximately the same. A slight decrease is noticed for the percentage of the point load with the increase of t/S. On the contrary, a slight increase occurs for the percentage of the frictional load with the increase of t/S. This is not mean the value of the point load decreases with the increasing in t/S but this results in the increasing in the frictional resistance of the pile which increase the total resistance of the pile and this decreases the percentage of the point load. However, the value of increasing in the percentage of t/S equal to 100% leads to very small value of increasing in the percentage of the skin friction resistances which may be less than the increasing from own weight of the raft.

Fig. 8 shows the relation between both point and frictional load of pile P11 and the total pile load of the same pile. It can be seen that, both of point and friction load increases with the increase of the pile load until a pile load equal to 154.0 tons, approximately (50%) of the pile load. After that, the frictional load becomes approximately constant and the point load increases approximately linearly with the progress of pile load. This means that, the increase in the friction load after 50% (approximately) of the pile load is very small. This indication that the friction stresses reach to level near the state of full mobilization at this pile load level.

Effect of the Contact between Soil and the Raft on Piles Loads

In the piled raft foundation the raft transmits the load to the piles and underneath soil (bedded cap). The contact pressure under raft is carried by the underneath soil. When a gap exists between the raft and the soil (free standing cap), the total load of the raft transmits to the piles only. Accordingly, all pile loads are increased in the case of free standing cap. Naturally, the existence of contact between the soil and raft decreases the piles load, as shown in Fig. 9. As can be seen in Fig. 9, the percentage decrease in the piles load lies in a range of 15-16%.

MOMENT ALONG THE PILE

Fig. 10-a and 10-b show the relation between t/S ratio and the absolute maximum value of Mx and My respectively. The maximum value of the bending moments

occurs at the connection between the pile and raft. It is seen that the values of the absolute maximum moment decrease with the increase of t/S ratio. In this respect, it is noted that when t/S ratio is doubled the moment value decreases to less that 40%. In other words, t/S ratio has a significant effect on the connecting moment between the pile and raft. Fig. 10 shows the distribution of bending moments Mx and My along the three piles P11, P13, and P33 for two values of t/S (0.24 and 0.48) when the uniform load (vertical load only) on the raft w=30.0 t/m2 or at Pt/Ptmax = 41%. As previously noted, the maximum value of Mx and My is at the piles heads. Increasing of t/S ratio reduces all values of bending moment at the piles heads, and increases slightly the moment in the middle of piles. This may be explained by the effect of the framing action that is assumed between the piles and raft. Of great importance, however, is the higher values of bending moments in the outer face of piles rather than inner faces. More specifically, as shown in Fig. 11 Mx and My at top of pile P11 as well as Mx at top of pile P13 are higher than those of the other faces of the considered piles. This conclusion can be generalized to all the piles under raft.

BENDING MOMENT AND DEFLECTION OF THE RAFT

Usually bending moment and deflection of the raft represents one of main objectives of the analysis for pile raft foundation design. In this section, the effect of the raft relative rigidity and the contact pressure under raft are studied.

Effect of the Raft Relative Rigidity on Bending Moment and Deflection of the Raft

Fig. 12 shows the distribution of bending moments on the raft, along sections A-A, and B-B, for four values of t/S (0.24, 0.32, 0.40 and 0.48) when Pt/Ptmax equal to 41% (raft load w=30.0 t/m²). It is observed that, the increase in the values of t/S increases all positives values of the bending moment of the raft. These values of the bending moment not only result from the uniform load on the raft but also result from the relative settlement of the supporting piles. So it very important to view the deflection of the raft along the supporting piles. Fig. 13 presents the deflection of the raft along sections A-A and B-B and shows the effect of raft relative rigidity t/S values on it when Pt/Ptmax equal to 41%. It is noted that, the value of raft relative rigidity t/S has a high influence on the deflection of the raft and the increasing in t/S value decreases the deflection. Also, this figure gives a good idea about the relative settlements of the piles and shows that, the relative settlement of the piles decreases with the increase in raft relative rigidity t/S.

Effect of Contact Pressure under Raft on Bending Moment and Deflection of the Raft

Fig. 14 shows the bending moment distribution on the raft for two cases. The first is the case of bedded cap (there is contact pressure between raft and soil). The second case is the case of free standing cap (there is a gap between raft and soil). It is noted that the absolute values of bending moment on the raft is less in the first case. Also, the deflection of the raft is less in the first case as shown in Fig. 15. It is very important to note that, the deflection in Fig. 15-a gives an idea about the relative settlement of the pile along section A-A.

CONTACT PRESSURE UNDER RAFT

The contact pressure under the piled raft may carry a significant amount of raft load. This is observed, in the model in which a gap is found between the raft and the soil (free standing cap). In that model, the

carrying capacity of the piled raft decreases by about 20%. In this section, some factors which may affect the contact pressure under raft are studied. However, the effect of the raft relative rigidity which is a function of the raft thickness and the pile spacing is included in this study.

Contact Pressure under Raft with the Progress of Loading

Fig. 16 presents the percentage of the resultant of the contact pressure under raft. It is noted that the percentage of the resultant of the contact pressure under raft increases with the progress of loading with a reasonable rate. Also, the raft relative rigidity t/S has little effect on the contact pressure under raft. This, in part, may be due to the increase of raft deformation with the progress of loading. Another reason is the settlement of the piles which cause the soil underneath the raft to be stressed by raft and the ability of the medium clay to carry the load.

CONCLUSIONS

A 3-D nonlinear finite element model for the analysis of concrete pile raft under vertical loading is presented. Both of the pile-foundation interaction and soil-foundation interaction has been taken into consideration. Based on the above study the following conclusions are highlighted:

1. The raft relative rigidity t/S affects the piles loads. The loads of the outer piles increase with the increase of t/S value, while whose of the inner piles decrease with the increase of t/S value.
2. Under the vertical load only the piles, in the concrete pile raft foundation, may be subjected to a significant amount of bending moment which has the maximum value at pile head.
3. The raft relative rigidity t/S has a high influence on the values of the maximum moment at the piles heads.
4. The increase in the values of the raft relative rigidity t/S increases all positives values of the bending moment of the raft.
5. The increase in the values of the raft relative rigidity t/S decreases the deflection of the raft and the relative settlements of the piles.
6. The resultant of the contact pressure under raft increases with the progress of loading by considerable rate and summation of contact pressure represents about 20% of the capacity of piled raft.

REFERENCES

1) Desai, C. S., Kuppusamy, T. and Alamddine, A. R. (1981) "Pile cap-Pile Group-Soil Interaction" ASCE, 107 (ST5), 817-834.

2) Abo-Ouf, A. M. (1992) "Analysis of Piled Raft Systems Supported on Nonlinear Soil Medium," Dr. Sc. Thesis, Faculty of Engineering, Cairo University.

3) Butterfield, R. and Banerjee, P. K. (1971). "The problem of pile group-pile cap interaction," Geotechnical, 21(2), pp. 135-142.

4) Poulos, H. G. and Davis, E. H. (1980). "Pile Foundation Analysis and Design." Wiley, New York. Sawko, F. (1968). "Simplified Approach to the Analysis of Piling System." The Structural Engineer, 46 (1), pp. 83-86.

5) Kuwabara, F. (1989), "An Elastic Analysis for Piled Raft Foundations in Homogeneous Soil."
Soil and Foundation, 29(1), pp. 82-92.

6) Sawko, F. (1968), "Simplified Approach to the Analysis of Piling System." The Structural Engineer, 46 (1), pp. 83-86.

7) Desai, C. S. and Holloway, D. M. (1972). "Load deformation analysis of Deep

Foundation." U.S. Army Engineers. Waterways Experiment Station. Mississippi.

8)Jeong, S., Kim, S., and Briaud, J., (1997), "Analysis of down drag on pile groups by finite element method" Computers and Geotechnics, 21(2), 143-161.

9) Shabana, W.A., "Analysis of raft foundation partially supported by pile columns". M.Sc. Thesis, Faculty of Engineering, Mansoura University, 2003.

10) Sharma, K. G. and Desai, C. S. (1992) "Analysis and Implementation of Thin-Layer Eleme

for Interfaces and Joints" Journal of Engineering Mechanics, vol. 118, pp. 2442-2461.

11)ANSYS 6.0, (2001), "ANSYS Structural Analysis Guide, Theory Reference." ANSYS, inc., Canonsburg.

12)Bathe, K. J. (1982), "Finite Element Procedures in Engineering Analysis" Prentice-Hall, Inc., Englewood Cliffs, New Jersey.

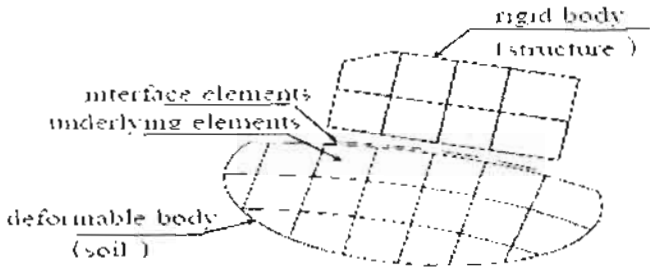

Fig. 1. Interface and Underlying Element

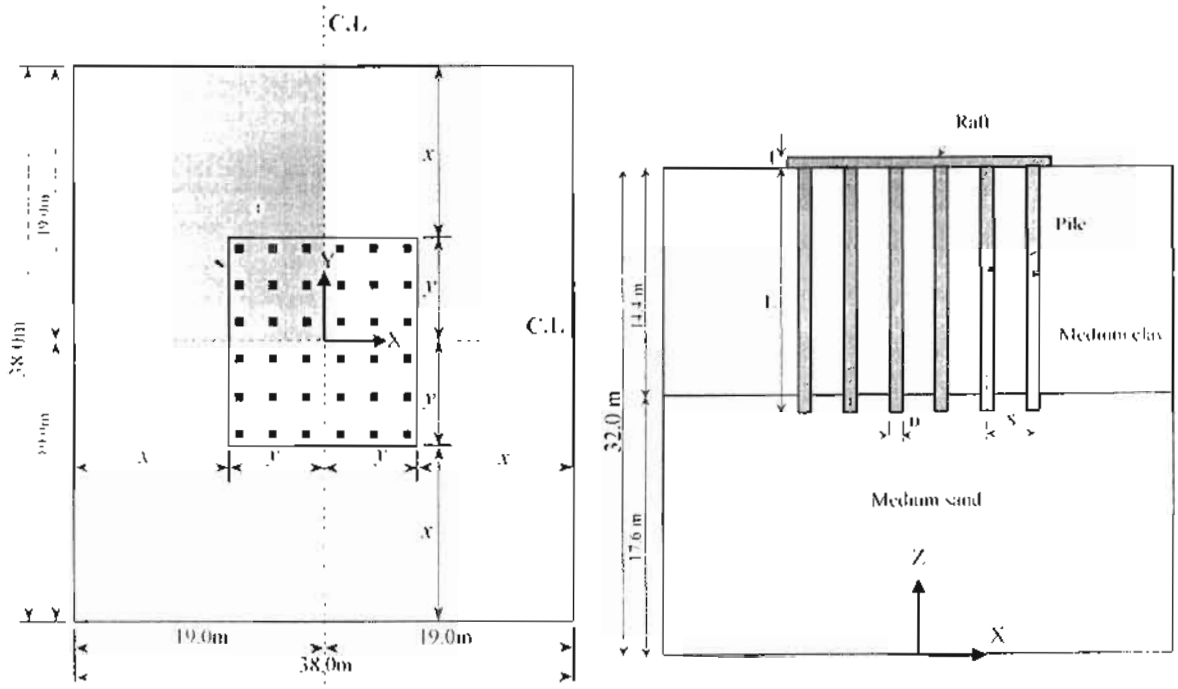

a) Plan b) Section elevation

Fig. 2. Geometrical dimension of the model

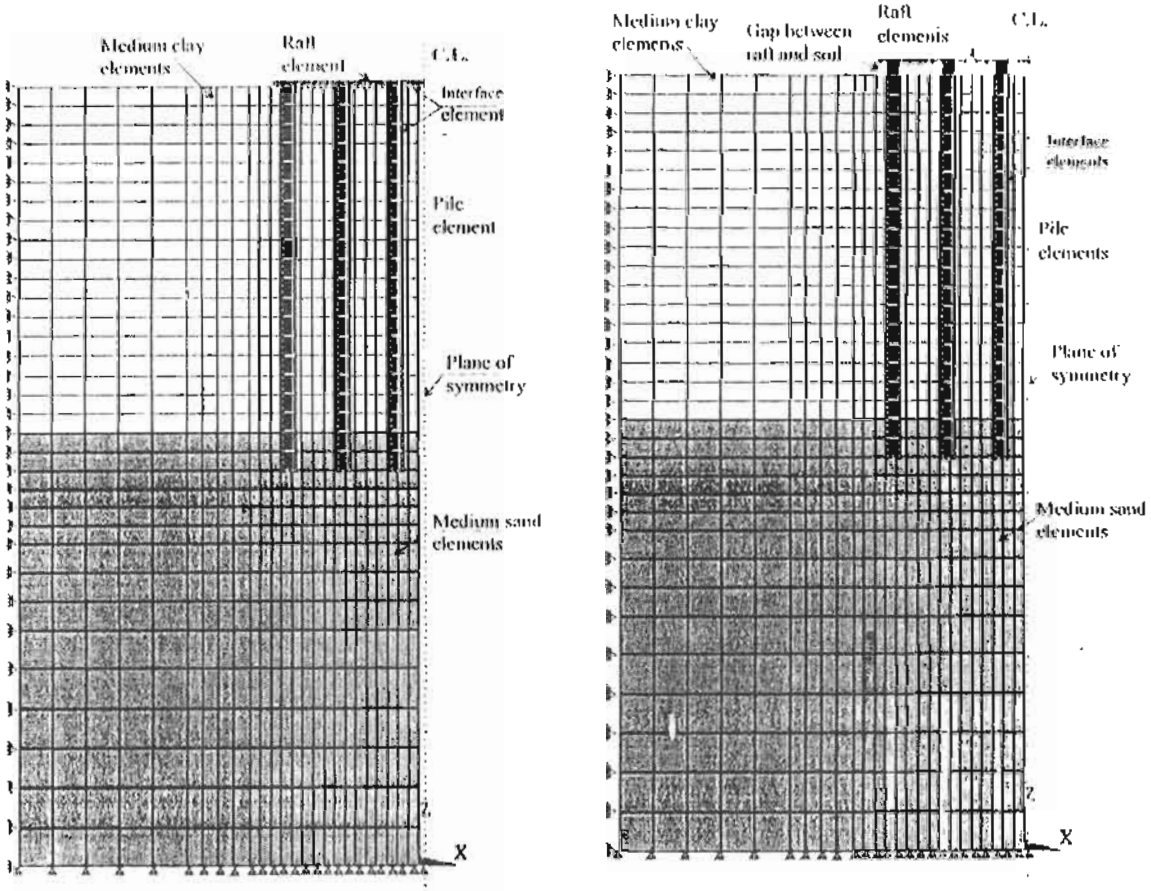

a) Contact pressure between raft and soil

b) Gap between raft and soil

Fig. 3. Meshing of the two models

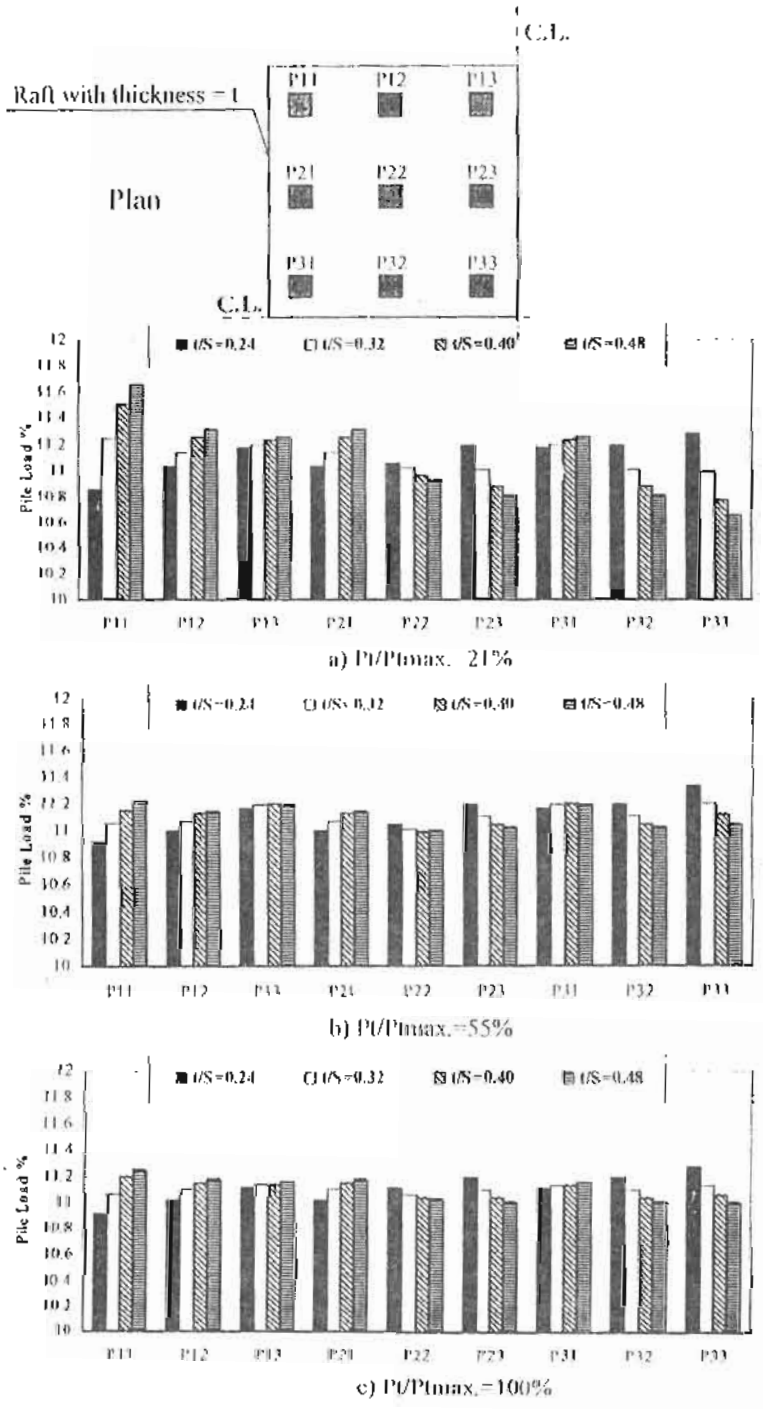

Fig. 4. Percentage of piles loads versus raft relative rigidity t/S

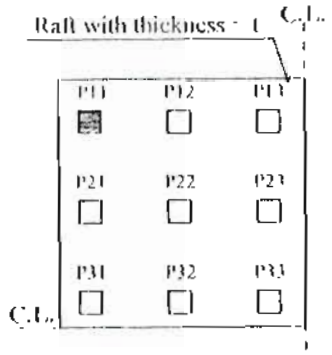

Plan

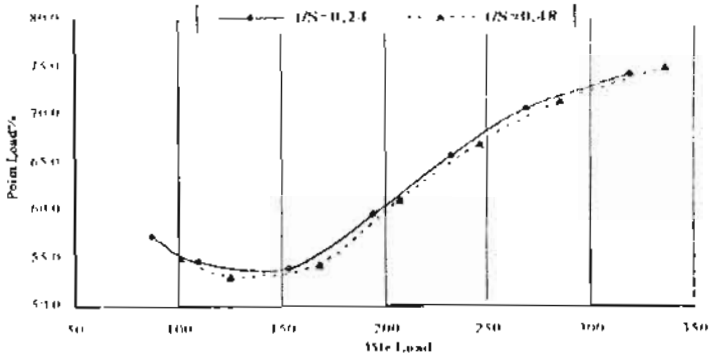

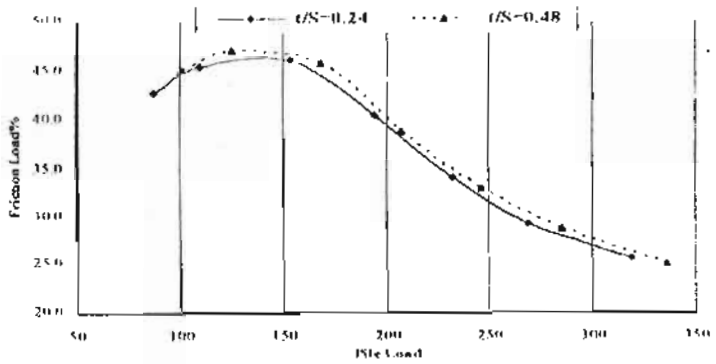

Fig. 5. Percentage of point load and frictional load for piles (P11) versus pile load for varies raft relative rigidity t/S

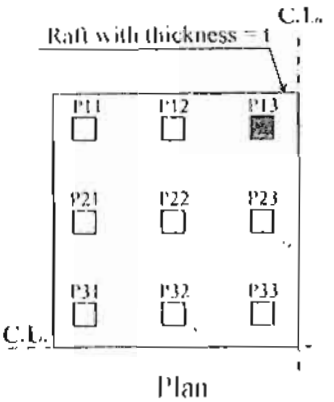

Plan

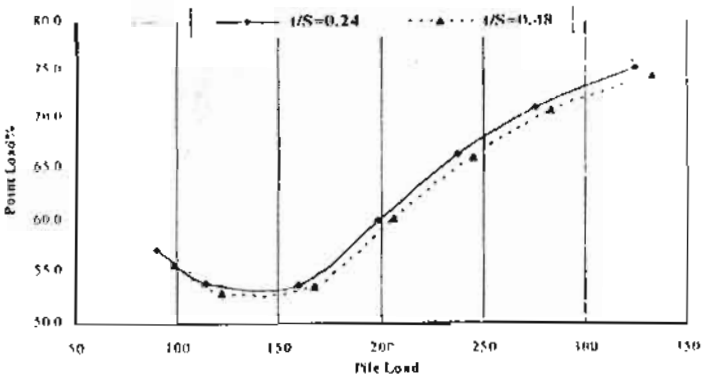

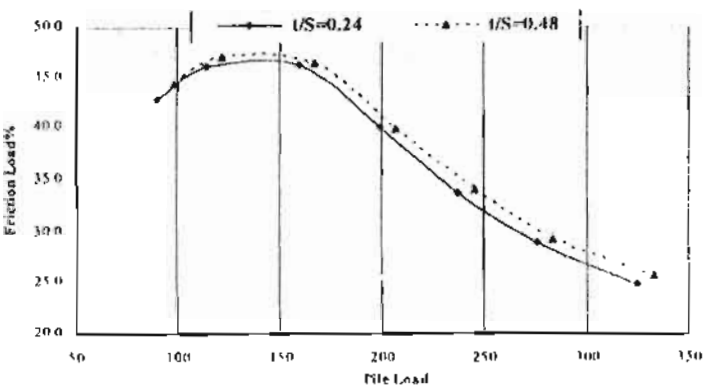

Fig. 6. Percentage of point load and frictional load for piles (P13) versus pile load for varies raft

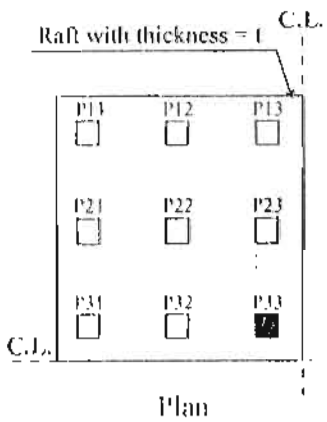

Plan

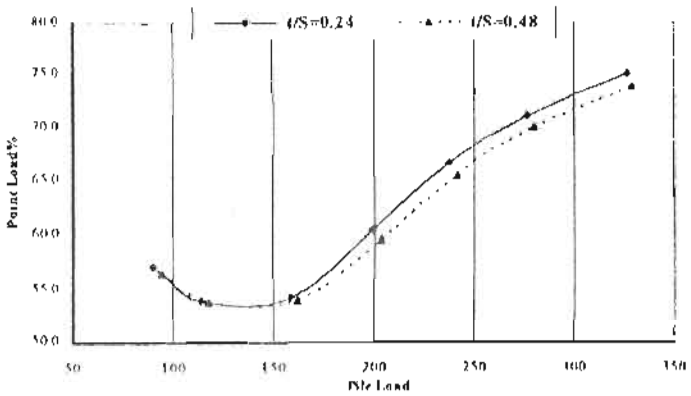

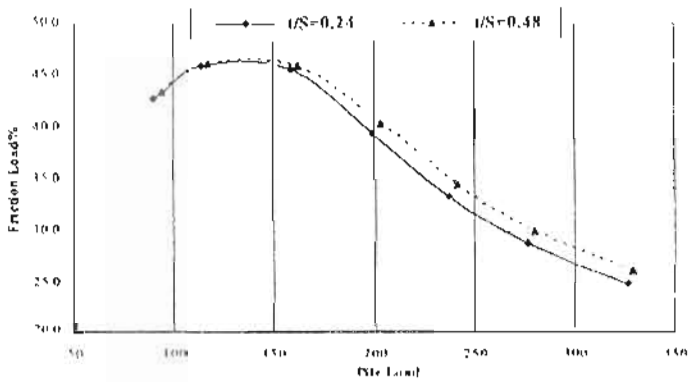

Fig. 7. Percentage of point load and frictional load for piles (P33) versus pile load for varies raft relative rigidity t/S

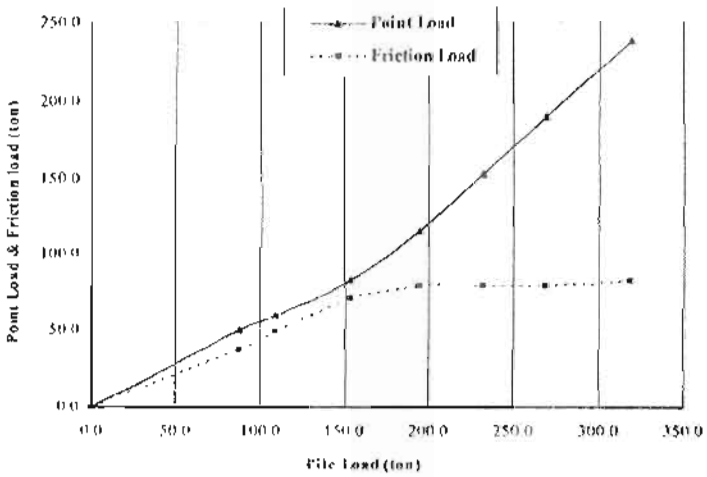

Fig. 8. Point and frictional load versus pile load for pile (P11)

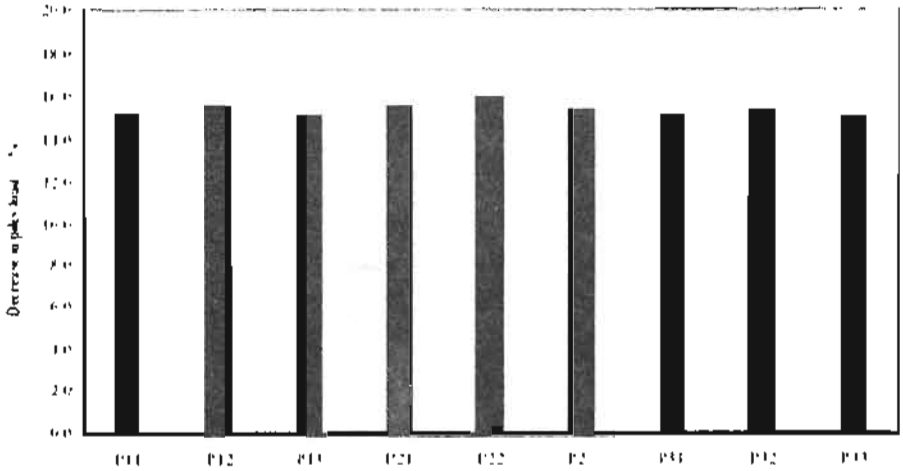

Fig. 9. Percentage decrease in piles load due to the contact between the soil and the raft

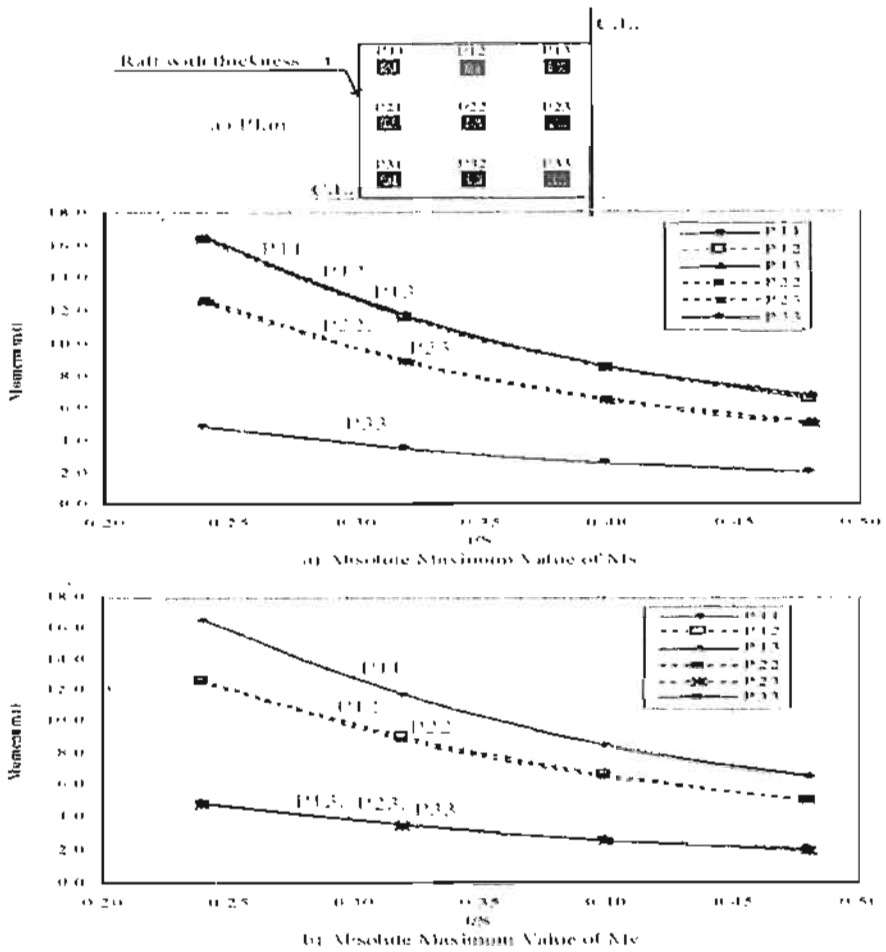

Fig. 10. Absolute maximum bending moment on piles (P11, P12, P13, P22, P23, and P33) versus raft relative rigidity t/S

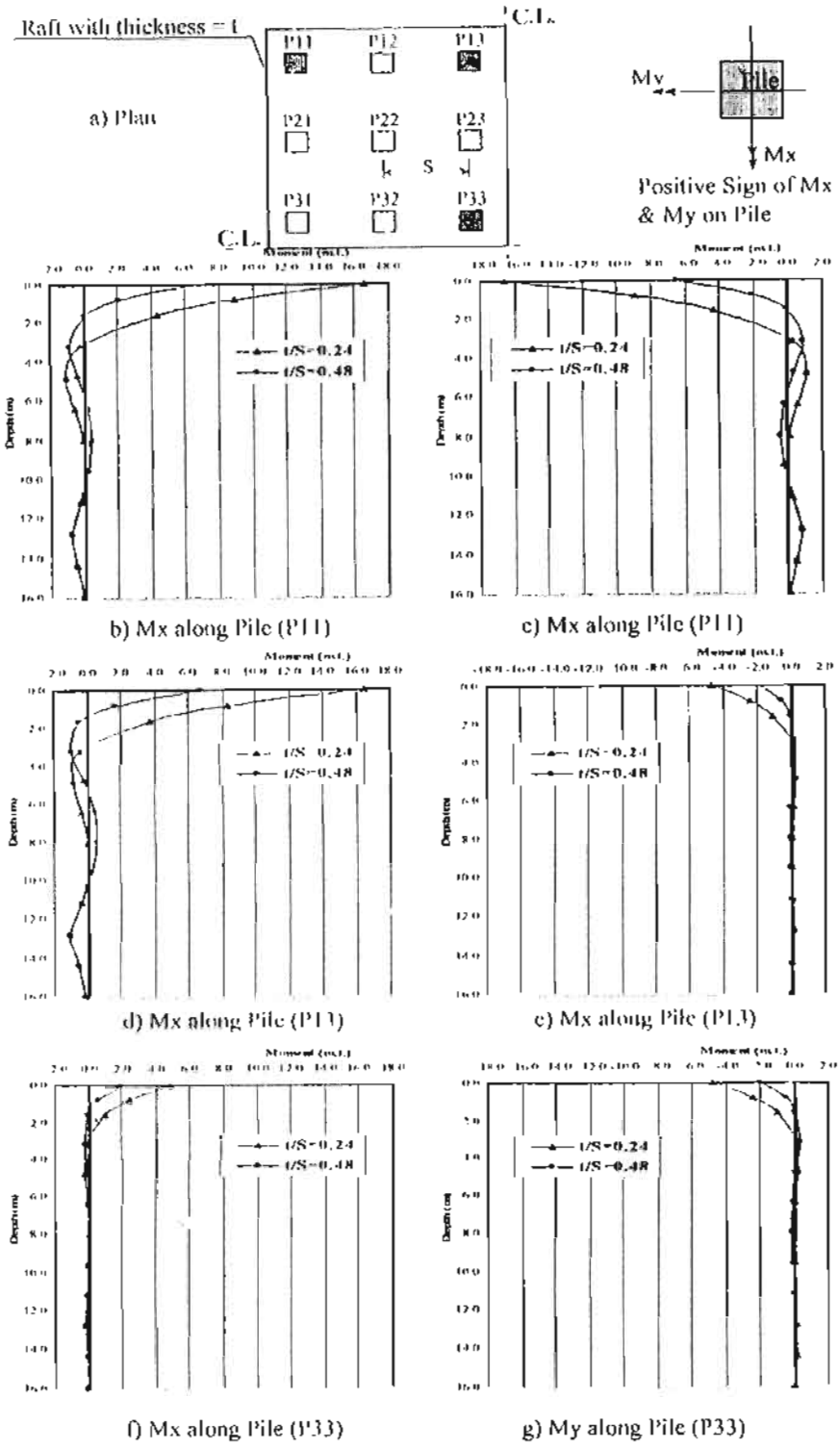

Fig. 11. Bending moment along piles (P11), (P13), and (P33)for t/S=0.24 & t/S=0.48 |Pl/Plmax=41%|

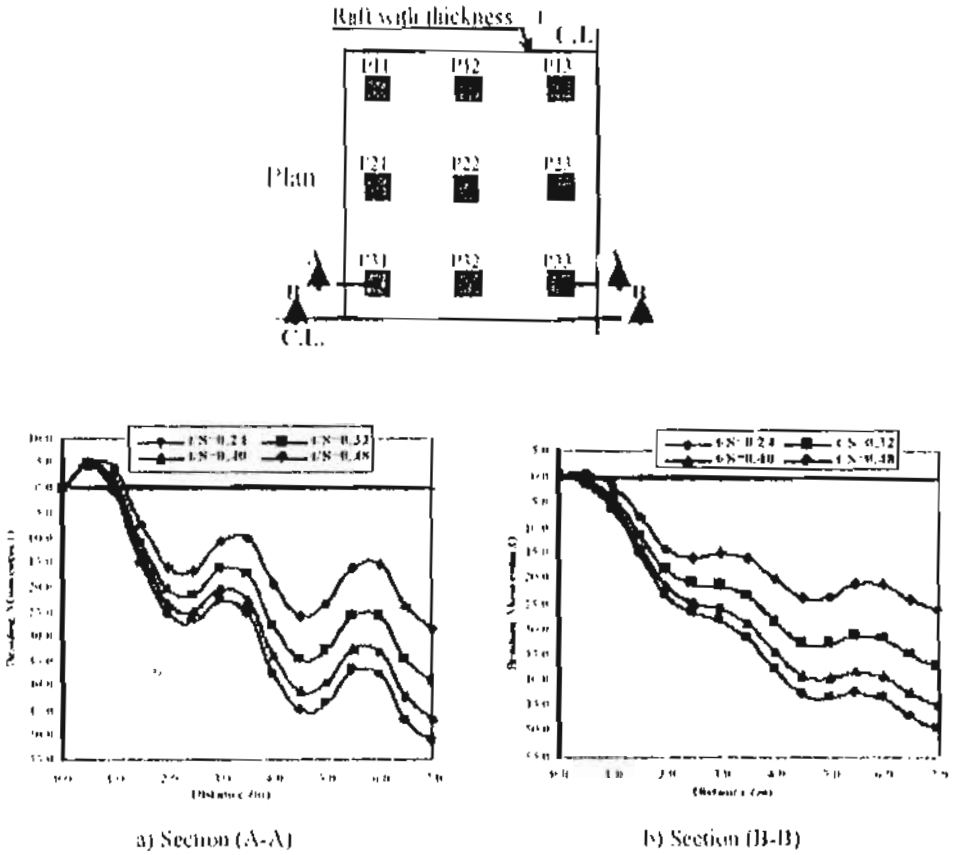

a) Section (A-A) b) Section (B-B)

Fig. 12. Effect of raft relative rigidity t/S on the Bending moment of the raft

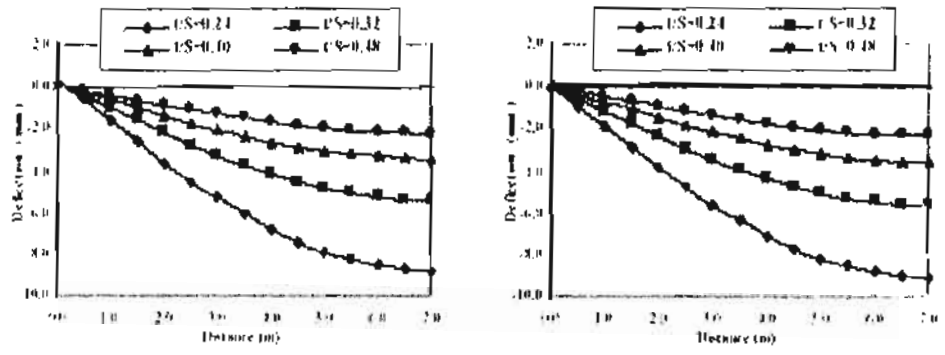

a) Section (A-A) b) Section (B-B)

Fig. 13. Effect of raft relative rigidity t/S on the deflection of the raft

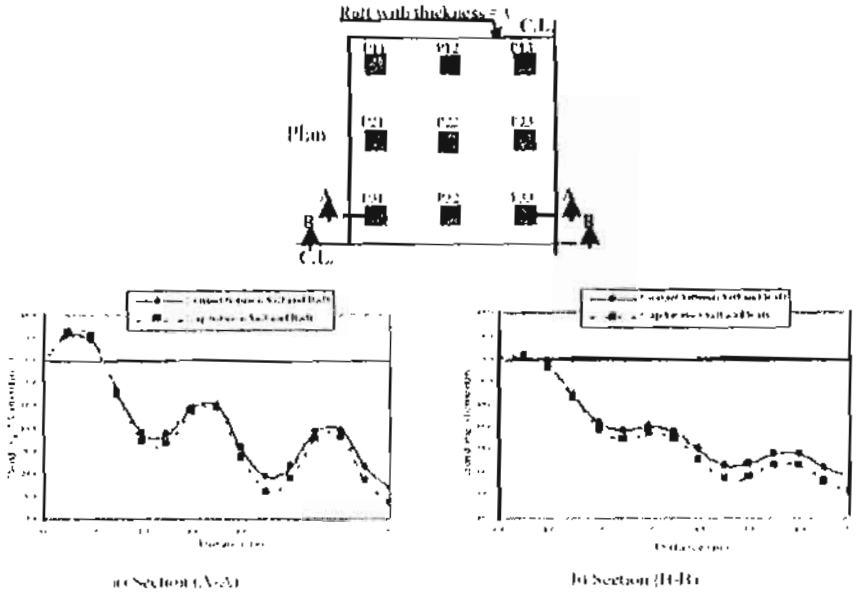

Fig. 14. Effect of contact pressure under raft on the bending moment of the raft

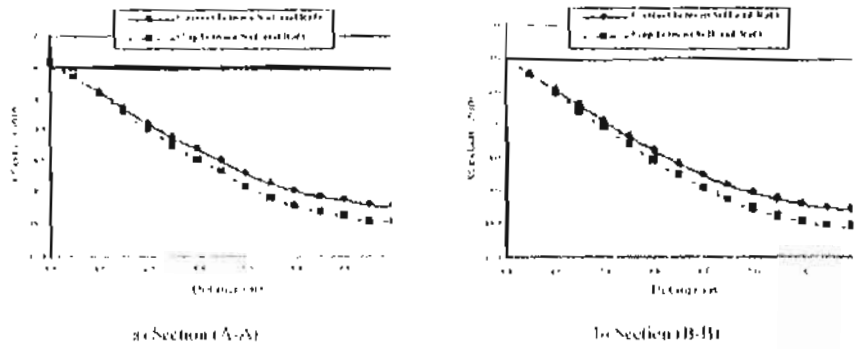

Fig. 15. Effect of contact pressure under raft on the deflection of the raft

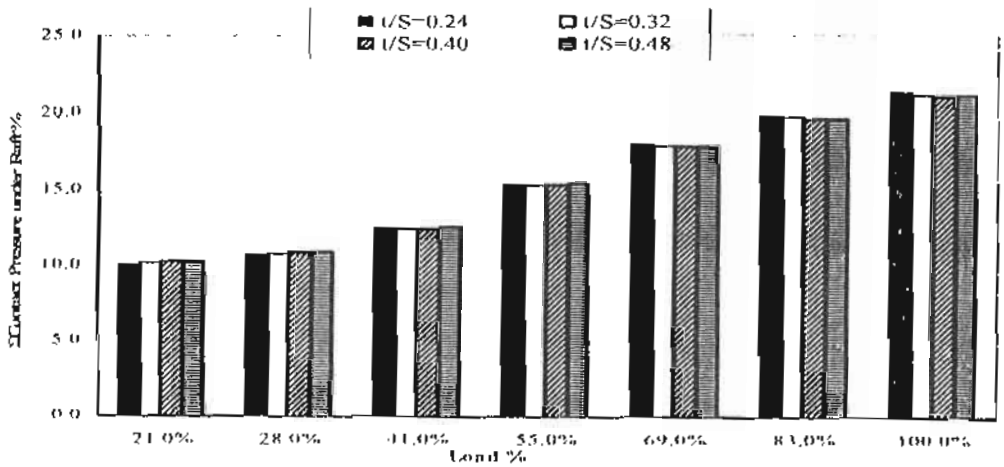

Fig. 16. Percentage of the resultant of the contact pressure under raft
Versus raft relative rigidity t/S with the progress of loading